Nondestructive evaluation of harvested cabbage texture quality using 3D scanning technology

Dongdong Du, Yongkai Ye, Dongfang Li, Jie Fan, Rob B.N. Scharff, Jun Wang, Fake Shan

PII: S0260-8774(24)00189-4

DOI: https://doi.org/10.1016/j.jfoodeng.2024.112123

Reference: JFOE 112123

To appear in: *Journal of Food Engineering*

Received Date: 28 November 2023

Revised Date: 17 April 2024

Accepted Date: 29 April 2024

Please cite this article as: Du, D., Ye, Y., Li, D., Fan, J., Scharff, R.B.N., Wang, J., Shan, F., Nondestructive evaluation of harvested cabbage texture quality using 3D scanning technology, *Journal of Food Engineering*, https://doi.org/10.1016/j.jfoodeng.2024.112123.

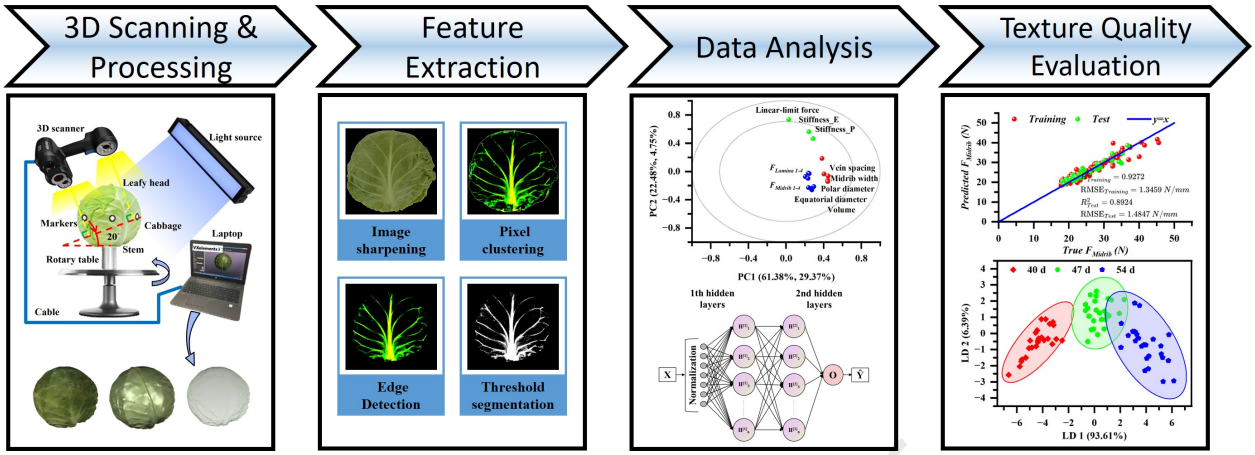

Running title: Nondestructive evaluation of cabbage texture via 3D scanning

Nondestructive evaluation of harvested cabbage texture quality using 3D scanning technology

Dongdong Du [a, b, d, ✉], Yongkai Ye [a], Dongfang Li [a], Jie Fan [b], Rob B.N. Scharff [c], Jun Wang [a, d], Fake Shan [a]

[a] *College of Biosystems Engineering and Food Science, Zhejiang University, 866 Yuhangtang Road, Hangzhou, 310058, PR China.*

[b] *Bioinspired Soft Robotics, Istituto Italiano di Tecnologia, Genova, 16163, Italy.*

[c] *Division of Integrative Systems and Design, The Hong Kong University of Science and Technology, Hong Kong, PR China*

[d] *Key Laboratory of Intelligent Equipment and Robotics for Agriculture of Zhejiang Province, Hangzhou, 310058, PR China.*

Abstract: Current nondestructive methods for evaluating the texture quality of leafy vegetables have limitations due to their complicated leafy structure. In this study, a promising solution was proposed using 3D scanning technology to nondestructively assess the texture quality of leafy vegetables, and the harvested cabbages were chosen as the experimental samples. The cabbages were scanned to extract the morphological traits, especially for surface features of vein distribution. Results demonstrated that morphological traits exhibited better correlations with texture indices compared to traditional compression features. Texture indices were well predicted based on the XGBoostR algorithm with high R^2 values of over 0.89 and low RMSE values. The texture quality of cabbages at different harvesting times analyzed by linear discrimination analysis also showed well-discriminative results with an accuracy exceeding 98.3%. These results successfully indicated that 3D scanning technology was effective in evaluating the texture quality of cabbages, showcasing its potential in the nondestructive texture evaluation of leafy vegetables.

Keywords: Nondestructive method; leafy vegetables; morphological traits; vein distribution; machine learning

✉ Corresponding author. Tel.: +86-15158132438; fax: +86-571-88208641.
E-mail addresses: dudd@zju.edu.cn (Dongdong Du).

1 Introduction

Texture is one of the most important quality attributes that greatly impacts consumers' preference for fresh fruits and vegetables (Li et al., 2023). For most fruits and vegetables, firmness often serves as the predominant method for assessing texture quality. However, when it comes to leafy vegetables like cabbages, the texture quality primarily relies on the fracture properties of the edible leaves (Watanabe et al., 2017), which are linked with their freshness and crispness, harvesting, processing, transporting, and storage (Zhang et al., 2022). In general, consumers often evaluate the texture quality of leafy vegetables by visually and tactilely inspecting them and rely on their subjective judgment to choose favorable ones. For objective evaluation, the commonly used puncture test employs physical indices such as maximum force, stiffness, and toughness, to describe the fracture properties of leafy vegetables by penetrating probes or blades (Gutiérrez-Rodríguez et al., 2013; Jaiswal and Abu-Ghannam, 2013; Retta et al., 2019). However, this objective evaluation of texture quality of leafy vegetables is destructive and not performed in real time. Hence, there is an urgent need to develop non-destructive and in situ methods for assessing the texture quality of leafy vegetables.

Among the various nondestructive methods for evaluating the texture quality, the acoustic vibration technique stands out as a commonly employed approach. This method employs an accelerometer (Mayorga-Martínez et al., 2016), piezoelectric transducer (Macrelli et al., 2013a, b), microphone (Fathizadeh et al., 2020), or laser doppler vibrometer (LDV) (Zhang et al., 2015) to nondestructively collect the vibration signals and evaluate the texture quality. The optical techniques, including visible/near-infrared/mid-infrared/hyperspectral imaging, have also been adopted as nondestructive methods to evaluate the texture quality by extracting featured spectral information (Liu et al., 2021; Pullanagari and Li, 2021; Yu et al., 2018). Both methods evaluate the texture quality (mainly referring to the firmness) of fresh fruits and vegetables based on the absorption, reflection, transmission, or scattering signals, which are suitable for pulpy fruits and vegetables such as apples, pears, potatoes, and tomatoes. However, leafy vegetables are different from these since they have a more complicated and heterogeneous leafy structure. This complexity makes the vibration and optical signals weak and difficult to extract, thus making evaluating texture quality a challenging work. For example, Zhang et al. (2021) attempted to evaluate the texture quality of Chinese cabbage using mechanical vibration, while Sánchez et al. (2018) attempted to evaluate spinach based on near-infrared spectroscopy. Both results were unsatisfactory due to the irregular leafy structure. The development of a non-

destructive method for assessing the texture quality of leafy vegetables remains an ongoing challenge.

The texture quality of leafy vegetables can be predominantly determined by the quality of their leafy structure. Botanists' previous studies have revealed that the texture quality of leafy vegetables is closely tied to the anatomical characteristics of plant leaves, particularly their leafy geometrical traits (Choong et al., 1992) and vein distribution (de la Riva et al., 2016). Therefore, leafy geometrical traits and vein distribution would serve as additional cues to characterize the texture quality of the leafy structure. These results indicated that 3D scanning technology would be a potential approach for evaluating the texture quality of leafy vegetables nondestructively by extracting their leafy geometrical traits and vein distribution. In the agriculture and food industries, the utilization of 3D scanning technology has proven valuable in acquiring geometrical parameters of products that correlate with other quality attributes. Adamczak et al. (2015, 2018) proposed a method combining 3D scanning technology and stichometry to evaluate the chemical composition of pork meat and predict the weight of chicken breasts, respectively. The 3D scanning technology was utilized to measure the volume of pork and the cross-sections of chicken breasts. This study revealed significant correlations between the chemical composition (water, protein, and fat content) and the meat density calculated by incorporating weight. Additionally, correlations were observed between the cross-sections of chicken breasts and their respective weights. Moreover, the 3D scanning method was successfully implemented to accurately distinguish blocks of *Octopus minor* exhibiting excess water absorption, achieving an impressive prediction accuracy of 88% (Han et al., 2020). These studies successfully extracted geometric characteristics, such as volume and area, directly from the 3D scanning models, yielding promising outcomes. However, limited research has been conducted on surface features, specifically the vein distribution of leafy vegetables. Hence, there is a need to develop a 3D-scanning-based method that can extract both the geometric traits and vein distribution of leafy vegetables for the evaluation of texture quality.

In this study, 3D scanning technology was utilized as a non-destructive method to evaluate the texture quality of leafy vegetables, and the harvested cabbages were selected as the experimental samples. The morphological traits (Ji-Shi et al., 2024) in this study, including geometrical traits and vein distribution, were extracted using advanced 3D scanning and processing algorithms. The correlations among morphological traits, compression features, and texture indices were revealed. Then, the prediction and discrimination of texture quality in cabbage samples were further utilized to exploit the underlying relationship. The main contribution of this study was firstly evaluating harvested cabbage texture quality based on 3D

scanning technology and showcasing the potential of 3D scanning technology in the non-destructive texture evaluation of leafy vegetables. This in-suite and non-destructive technology for texture evaluation could be an efficient solution to grading harvested leafy vegetables in the production line.

2 Materials and methods

2.1 Materials

Due to the popularity and extensive commercialization, plants of the transplanting cultivar 'Lanzhou' with uniform head size were selected for the experiments. To analyze the variation in the texture quality of cabbage, fresh samples were carefully picked from the local fields in Hangzhou (Zhejiang, China) and collected in three sections at 7 d intervals (40 d, 47 d, and 54 d after transplanting). Finally, a total of 75 cabbage samples without visible damage (25 samples for each harvesting time) were randomly selected. Once the harvested cabbage samples arrived at the laboratory in Zhejiang University within 2 h each time, they were then immediately conducted for subsequent experiments at room temperature (20 ± 2 °C) and 80% (±2%) relative humidity, including weight measuring, 3D scanning and processing, compression, and texture quality tests. All the experiments were completed on the second day of arrival. The weight was measured by an electronic balance (FB-21153, Aminno Co., Ltd, Huzhou, China) with a precision of 0.01 g. The values (mean ± std) of the mass were 496.28 ± 87.01 g, 1129.48 ± 178.05 g, and 1196.88 ± 254.85 g, respectively, at the three harvesting times.

2.2 Morphological traits determination

In this study, morphological traits of each cabbage sample comprised five features: equatorial diameter, polar diameter, volume, midrib width, and vein spacing. To obtain the morphological traits of harvested cabbages, 3D scanning tests were performed on a customized testing platform, as shown in Fig. 1a. A full-color scanning portable 3D scanner (Go!Scan 50, Creaform Inc., Lévis, Canada) was set at approximately 20° slant plane from the horizontal ground on a ball head tripod and linked to a laptop. The set scanning slant angle could ensure comprehensive details and high scanning efficiency (Satric et al., 2024; Uyar and Erdoğdu, 2009). The scanner can do 3D full-color scanning using only white light (Visible light, wavelength from 380-750 nm) with an accuracy of 0.1 mm, which is based on structured light triangulation technology, using a combination of white light projection and camera capture to obtain the 3D object (Geng, 2011).

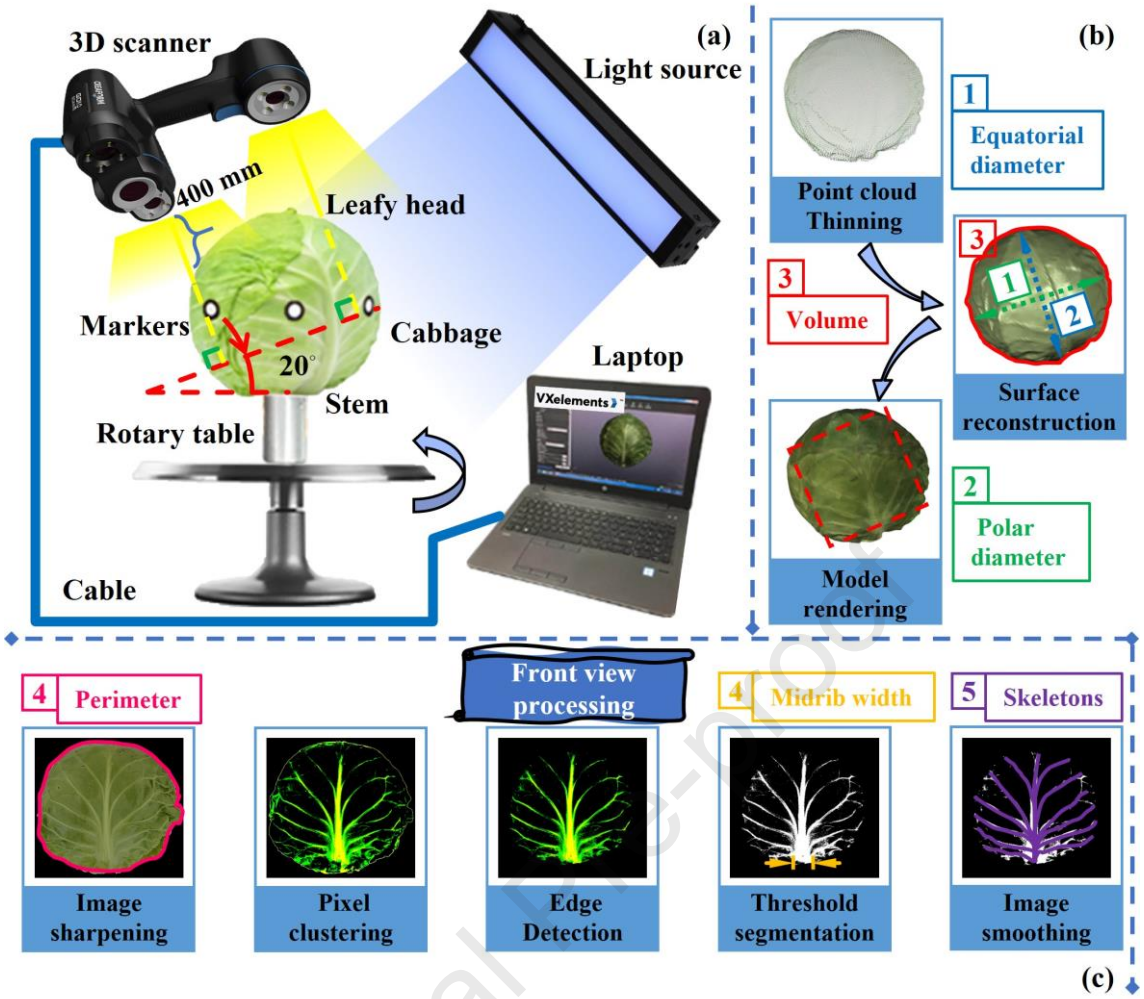

Fig. 1. (a) The schematic of the 3D scanning experimental setup. (b) Point cloud processing procedure, including point cloud thinning treatment, surface reconstruction, and colorful 3D model rendering. The green and blue arrows showed the measurements of equatorial and polar diameter, respectively, while the red curve and dashed rectangle marked part showed the measurements of volume and the front view of the rendered cabbage sample, respectively. (c) Vein feature extraction, includes five steps, image sharpening, pixel clustering, edge detection, threshold segmentation, and image smoothing. The magenta curve marked part, the orange line marked part, and the purple curves marked part were the perimeter of the front view, midrib width, and skeletons, respectively. (Appear in color online only)

Scanning tests were conducted within the scanning field of 380 mm × 250 mm × 380 mm (height × depth × width) at a resolution of 0.5 mm. During the tests, each cabbage sample was placed on a laboratory-made rotary table, and a white light source (EF-B-327L-W, Rsee Inc., Dongguan, China) was hung above the sample to ensure a suitable light environment. The distance between the 3D scanner and the cabbage was precisely measured to be 400 mm (Stand-off distance). To obtain better 3D scanning results, the scanning process was divided into two steps for every sample. First, with the root of the sample

placed on the rotary table (stem down), the leafy head part of the cabbage was scanned. Subsequently, the sample was turned upside down to scan the stem part (head down). During each step, a total of 15-25 positions were carefully captured, and duplicate scanning was also carried out for each step three times to avoid incomplete collection. Each sample took about 3 min to complete the 3D scanning procedure. Six identical sticky markers were unevenly distributed on the side surface around the equator of each sample to help the software align and fuse the two captured scanned parts. In particular, the markers were also used for determining the front view of the cabbage samples with two markers specially attached to both sides of the front view. After scanning, the generated raw point cloud, consisting of a series of 3D points with position information and a color map and consisting of a series of 3D points with position information and a color map to reshape the surface of the scanned cabbage sample, was processed by a highly integrated 3D measuring software (VXelements, Creaform Inc., Lévis, Canada).

As illustrated in Fig. 1b, after the initial generation of the raw point cloud with the portable 3D scanner, it underwent a series of processing steps. These steps involved the removal of artifacts, such as points affected by light reflection and unrelated objects (e.g., the rotation table piece). Additionally, a linear algorithm with a simplification value of 2 mm, was applied to thin out the point cloud by eliminating redundant points for facilitating further data processing. Therefore, approximately 40,000 points were preserved to reconstruct the bounded solid shape using triangular surface patches. Subsequently, a rendered 3D model was generated using the reconstructed solid, showcasing detailed morphological characteristics of the sample. The geometrical traits, including equatorial diameter, polar diameter, and volume, were then extracted from the rendered model using the 3D measuring software, where the equatorial diameter and polar diameter were acquired utilizing the oriented bounding volume method (Jang et al., 2014), while the volume was calculated using the Point Cloud Library.

Further, the front view of the 3D rendered cabbage (red dashed rectangle marked part in Fig. 1b, resolution: 1280 × 960 pixels) was extracted by ensuring the position of the two special markers and projecting the rendered 3D model and then processed to extract the surface features of vein distribution. To obtain the vein distribution, the front view was processed by a feature extraction algorithm shown in Fig. 1c, comprising general image processing algorithms (Gonzalez et al., 2004), a contour finding algorithm, and a skeleton extraction algorithm. The contour finding algorithm utilized the FindContours function in the OpenCV Library to obtain the perimeter, while the skeleton feature extraction algorithm was based on a

universal algorithm for image skeletonization (Saeed et al., 2010). The feature extraction algorithm was run in an available Integrated Development Environment (Microsoft Visual Studio 2017, Microsoft Corporation, Redmond, USA), including five steps:

Step 1: Image sharpening. For the front view, it was challenging to identify clear differences at the junction between veins and lamina, which made further image segmentation difficult. To address this issue and enhance the edge information of cabbages, the three-order Laplacian operator (Equation (1)) was applied by performing one convolution operation on the captured front view. Afterward, the obtained result was further processed using the contour finding algorithm to accurately extract the perimeter of the front view.

$$\mathbf{H} = \begin{bmatrix} 0 & 1 & 0 \\ 1 & -6 & 1 \\ 0 & 1 & 0 \end{bmatrix} \quad (1)$$

Step 2: Pixel clustering. A pixel clustering method based on color features was utilized for the pre-segmentation of the vein distribution. The pixels were efficiently grouped into their respective color categories by introducing two RGB color vectors and calculating the Euclidean distances between them. First, three-dimensional target RGB vectors T_k (R, G, B) (k = 0, 1,⋯, 7) were introduced to label the eight target color categories, including black, blue, green, cyan, red, magenta, yellow, and white. Second, the current color of each pixel was designated with its pixel RGB vector $C_{(i,j)}$ (R, G, B) (i = 0, 1, ⋯, h; j = 0, 1,⋯,w). For each pixel, the Euclidean distances between pixel RGB vector $C_{(i,j)}$ and target RGB vectors T_k were calculated. The target color, which corresponded to the shortest distance, was selected as the color category for the current pixel.

Step 3: Edge detection. To enhance the extraction accuracy of vein distribution and mitigate the impact of noise information caused by water stains around the edge of the cabbage leaves, a three-order Canny operator was applied. It effectively trimmed 10% of the area along the leaf profile.

Step 4: Threshold segmentation. The traditional Otsu threshold segmentation method was adopted for post-segmentation of the vein distribution (Otsu, 1979). The image was then binarized by the obtained threshold and processed to extract the midrib width by ensuring the length of the bottom pixels.

Step 5: Image smoothing. The median filtering method was employed with a kernel size of three to eliminate isolated noise points resulting from the binarization process. Subsequently, all connected regions were detected, and the bottom 10%

of regions were excluded based on their area values. The skeletons were extracted within the smoothing image using the aforementioned algorithm. Then, the vein spacing was calculated by Equation (2).

$$Vein\ spacing = \frac{Perimeter - midrib\ width}{Number\ of\ skeleton + 1} \quad (2)$$

2.3 Compression features acquisition

Compression tests were conducted to assess the physical compactness of cabbages, serving as a control method for evaluating the texture quality (Zhang et al., 2022) and performed using a commercial texture analyzer (TMS-PRO, Food Technology Corporation, Virginia, USA) equipped with a 75 mm diameter plate (see Fig. 2a). Each cabbage sample was compressed at the equatorial surface at a speed of 5 mm/min, applying a 20% deformation of the equatorial diameter (Li, 2013). The compressive force-displacement curves were recorded to extract the compression characteristics. Fig. 2b displayed three typical curves obtained from three cabbage samples harvested at different times. The curves showed that the compressing force of the cabbage was greater at the later harvesting time compared to the early harvesting time (Gil et al., 2012). The compressing force initially exhibited non-linear growth, transitioning to linear growth after a brief time interval. This period was regarded as the elastic region where the deformation was reversible and could be fully recovered. However, once the deformation entered the plastic phase, a distinct linear limit point was observed (black points marked part in Fig. 2b). Beyond this point, the compressing force continued to increase linearly, albeit at a slower rate. During this period, the deformation became permanently plastic, meaning it could no longer be recovered. According to Zhang et al. (2015), the following parameters were extracted from the curves as the compression features: (1) F_{ll} (Linear limit force), the compressing force at the linear limit point; (2) Stiff_E (Stiffness at elastic region), the slope of the curve before linear limit point; (3) Stiff_P (Stiffness at plastic region), the slope of the curve after the linear limit point. Stiff_E and Stiff_P were calculated by Equations (3) and (4).

$$\text{Stiff\_E} = \frac{F_{ll} - 50\%F_{ll}}{d_2 - d_1} \quad (3)$$

$$\text{Stiff\_P} = \frac{150\%F_{ll} - F_{ll}}{d_3 - d_2} \quad (4)$$

where F_{ll} was the linear limit force (N), d_1 was the displacement at 50% F_{ll} before the linear limit point (mm), d_2 was the displacement at F_{ll} (mm), and d_3 was the displacement at 50% F_{ll} after the linear limit point (mm).

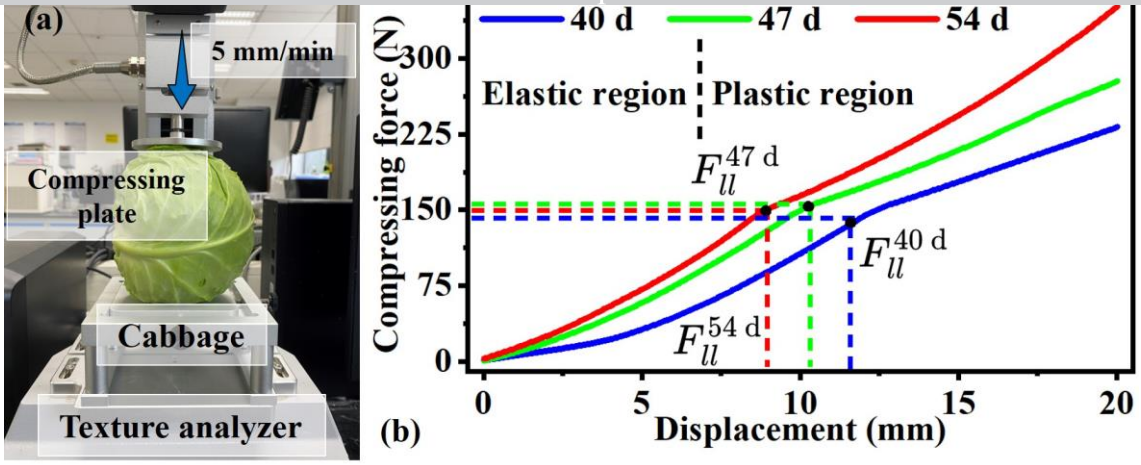

Fig. 2. Compression test setup and feature acquisition. (a) Experimental setup for the compression test. (b) Typical compression curves of the cabbage samples at three harvesting times for feature acquisition. The black points marked part was the linear limit point, and the compressing force at this point represented the linear limit force F_{ll}. (Appear in color online only)

2.4 Texture indices extraction

Fracture properties of the edible leafy part, comprising both the lamina and midrib, were typically examined to assess the texture quality of harvested cabbages. These properties were then employed in conducting puncture tests using the aforementioned texture analyzer. As shown in Fig. 3a, the texture analyzer was equipped with a 1 kN load cell and a flat Warner-Bratzler blade at a downward speed of 50 mm/min (Jaiswal et al., 2012). The puncture test was conducted until the blade penetrated the laminas and midribs. To quantitatively assess the texture quality of the cabbage samples, the texture curves of both laminas and midribs were measured to derive the corresponding texture indices. Due to the difference in dimensions, the lamina and midrib samples were extracted from the four outermost leaves of the cabbage specimens. The laminas were cut collectively, while the midribs were cut individually, from the outermost to the innermost layers. Based on the cutting arrangement of leaves in the cabbage samples, the laminas and midribs were labeled numerically, ranging from lamina 1 to lamina 4 and from midrib 1 to midrib 4, respectively. The texture quality curve of the laminas, as illustrated in Fig. 3b, displayed four prominent peaks in the cutting force-displacement curve for each laminar layer during the test. As the blade penetrated the leaves, there was a gradual reduction in the cutting peak force, implying that the outer leaves possessed superior texture quality compared to the inner leaves. The cutting peak forces of the four laminas, including $F_{Lamina\ 1}$, $F_{Lamina\ 2}$, $F_{Lamina\ 3}$, and $F_{Lamina\ 4}$, were selected as the texture indices for laminas. The same changing tendency can also be observed

in the results of typical texture quality curves of midribs shown in Fig. 3c. Throughout the entire puncturing process, the cutting force progressively increased, reached a peak, and rapidly decreased to its minimum for each midrib. Similarly, the cutting peak forces of the four midribs, including $F_{Midrib\ 1}$, $F_{Midrib\ 2}$, $F_{Midrib\ 3}$, and $F_{Midrib\ 4}$, were extracted as the texture indices for midribs. Finally, the texture indices were $F_{Lamina\ 1}$, $F_{Lamina\ 2}$, $F_{Lamina\ 3}$, and $F_{Lamina\ 4}$ for lamina texture quality and $F_{Midrib\ 1}$, $F_{Midrib\ 2}$, $F_{Midrib\ 3}$, and $F_{Midrib\ 4}$ for midrib texture quality.

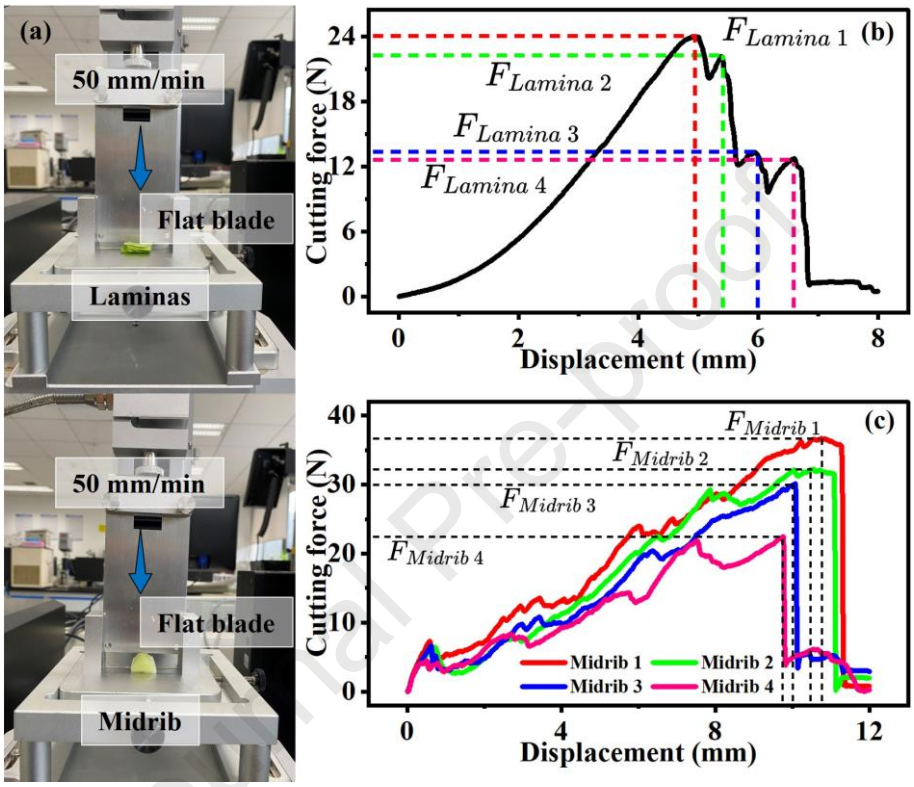

Fig. 3. Texture quality test setup and texture indices extraction. (a) Experimental setup for measurement of the lamina and midrib texture quality. (b) Typical texture quality curve of the laminas. (c) Typical texture quality curves of the midribs. (Appear in color online only)

2.5 Statistical analysis

Multivariate data analysis was applied for the evaluation of texture quality. First, a one-way analysis of variance (one-way ANOVA) was employed to show the variations in morphological traits, compression features, and texture quality at three harvesting times. Significant differences between cabbage samples within the same group were indicated by distinct letters. (Tukey test with a significant level of 0.05). Second, correlation analysis (CA) and ANOVA-partial least squares regression (APLSR) were utilized to assess the viability and effectiveness of utilizing morphological traits in determining texture quality. CA, a statistical method used to measure the strength of correlation between two or more quantitative variables, was employed.

The correlation coefficients with a significance level of 0.05 were utilized for quantifying the relationships. APLSR was employed to conduct a detailed analysis of the correlation between independent variables and dependent variables. By modeling latent variables that represented the primary shared variance among the variables, APLSR effectively mitigated multi-collinearity problems (Gu et al., 2019). Jack-knifing was utilized to estimate the approximate variance of the regression coefficient at a significance level of 0.05 and determine the significance indications revealed in the quantitative APLSR analysis.

Furthermore, to conduct a detailed quantitative analysis of the texture quality, various regression methods such as partial least squares regression (PLSR), polynomial regression (PR), support vector regression (SVR), and extreme gradient boosting regression (XGBoostR) were utilized. PLSR, a powerful multi-linear regression technique, plays a crucial role in establishing linear relationships between independent and dependent variables. By integrating the strengths of principal component analysis, multiple linear regression, and analysis of variance, PLSR excels in effectively addressing multicollinearity challenges (Guebel and Torres, 2013). PR is an algorithm that employs polynomial functions as independent variables to generate nonlinear equations (Dean et al., 2017), which has the added advantage of easily approximating the measured point by raising the order. SVR is regarded as one of the most robust and accurate regression methods due to its implementation of an efficient support vector (Awad and Khanna, 2015). In the experiment, the Gaussian radial basis function (RBF) was chosen as the kernel function for its strong overall performance and minimal parameter requirements. The determinations of kernel parameter *gamma* and penalty factor *C* significantly impact the performance of the SVR algorithm. XGBoostR, a popular ensemble learning algorithm, garners significant attention due to its remarkable training speed and superior accuracy, possessing several advantageous characteristics, of being resilient against overfitting, being robust to outliers, and the excellent anti-noise capabilities (Chen and Guestrin, 2016). The central idea of this algorithm is to fit the residuals between the predicted and true values in the last round. To achieve the optimization of these algorithms, the approach of grid search was introduced (Bergstra and Bengio, 2012). The optimized hyper-parameters of the selected algorithms are listed in Table 1. The performance of prediction was evaluated by coefficient of determination (R^2) and root mean square error (RMSE). The larger R^2 and the lower RMSE values would indicate better prediction performance.

Finally, principal component analysis (PCA) and linear discriminant analysis (LDA) were employed for the texture

quality discrimination. PCA is a powerful unsupervised multivariate statistical method used to analyze the underlying structure of an original dataset. Its primary objective is to reduce dimensions by projecting the high-dimensional dataset onto a lower-dimensional subspace that captures a significant portion of the variance in the original dataset. LDA is another well-known statistical method utilized to identify new lower-dimensional variables that exhibited strong discriminatory power within the original dataset. In contrast to PCA, LDA is a supervised approach that not only detects the dispersion of data points within the same category but also considers the separation between different categories. The performance of discrimination was assessed by observing the clustering degree and classified accuracy.

Table 1 Optimized hyper-parameters of the selected machine learning algorithms

Algorithm	Hyper-parameter	Value
Partial least squares regression	*Number of the components*	5
Polynomial regression	*Max order of the polynomial*	4
Support vector regression	*Kernel function*	'rbf'
	Kernel parameter gamma	0.3
	Penalty factor C	11
Extreme gradient boosting regression	*Max depth*	4
	Learning rate	0.09
	Number of estimators	100

In this study, the total dataset comprised 75 samples and was evenly divided into three groups based on the harvesting time. During the supervised modeling phase, each group's dataset was further divided into two subsets. The training set consisted of 20 randomly selected samples, while the testing set comprised the remaining 5 samples. Subsequently, the training and testing sets from the three groups were combined to form a new training set and a new testing set, respectively. Consequently, the final training set consisted of 60 samples, while the testing set comprised 15 samples. The data processing methods, including CA, APLSR, PLSR, PR, SVR, XGBoostR, PCA, and LDA, were implemented in Python 3.8.3.

3 Results and discussion

3.1 Measurement of morphological traits, texture indices, and compression features

3.1.1 Morphological traits

Results of morphological traits extracted by the proposed 3D scanning and processing method are shown in Fig. 4. All the morphological traits progressively increase with the increase of the harvesting time, and significant differences are observed in most morphological traits, except for the vein spacing between 47 d and 54 d. The phenomenon is related to the

increase of leafy structure with the cabbages ripening (Gil et al., 2012). The volume (Fig. 4c) and midrib width (Fig. 4d) exhibit a relatively consistent increase in the magnitude. For the features of equatorial diameter, polar diameter, and vein spacing shown in Figs. 4a, 4b, and 4e, respectively, the magnitude of increase during the period from 40 d to 47 d exceeds that of the period from 47 d to 54 d. Because the size of the cabbage head increases and eventually stabilizes at a horticultural maturity as the cabbages grow (Radovich et al., 2004). Particularly for vein spacing, the differences become progressively smaller as the cabbages mature, which is due to the compact leafy structure formed by the stacking of multiple leaves, causing stable and complex changes in physiochemical properties (Zhang et al., 2021).

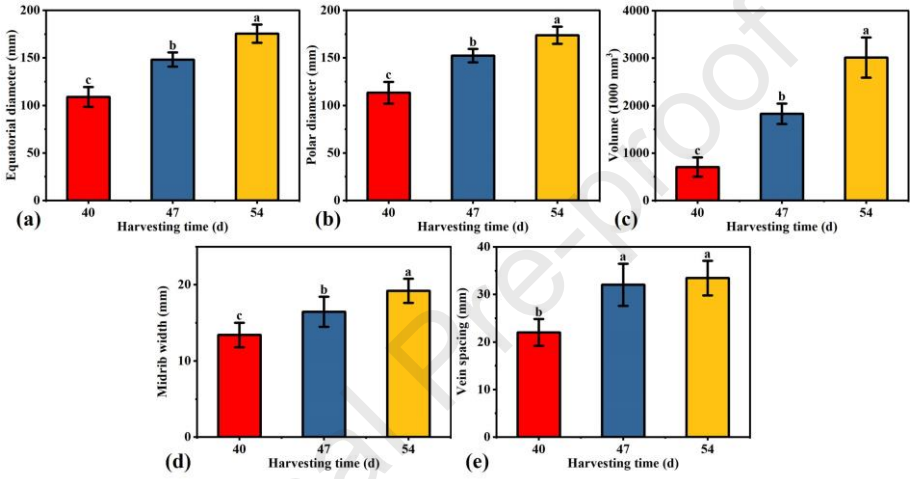

Fig. 4. Morphological traits measurements. Variation of (a) equatorial diameter, (b) polar diameter, (c) volume, (d) midrib width, and (e) vein spacing. (Appear in color online only)

3.1.2 Compression features

Compression feature acquisition results shown in Fig. 5a indicate that there is no significant difference in the linear limit force (F_{ll}) among the three harvesting times. As the harvesting time increases, the linear limit force exhibits a pattern of initially increasing and then decreasing. The change that occurs on 47 d is a result of the increase in compactness, which results in a reduction in the percentage of recovery (Gil et al., 2012). Results between 47 d and 54 d prove again that the cabbages harvested at a later stage required enhanced protective measures to prevent plastic deformation and cracking damage (Holt and Schoorl, 1983) for the lower the linear limit force means the greater the possibility that the cabbages suffer plastic deformation (Zhang et al., 2021). In terms of stiffness (Fig. 5b), both Stiff_E and Stiff_P show an increasing trend as the harvesting time increases. Notably, Stiff_E exhibits significantly higher values than Stiff_P for the samples harvested at the same time. However, the increase in both Stiff_E and Stiff_P is discernible but not pronounced. This reason is that the stiffness

could be mainly influenced by the head density, which tends to stabilize due to the linear correlation between head weight and volume (Theodore et al., 2005).

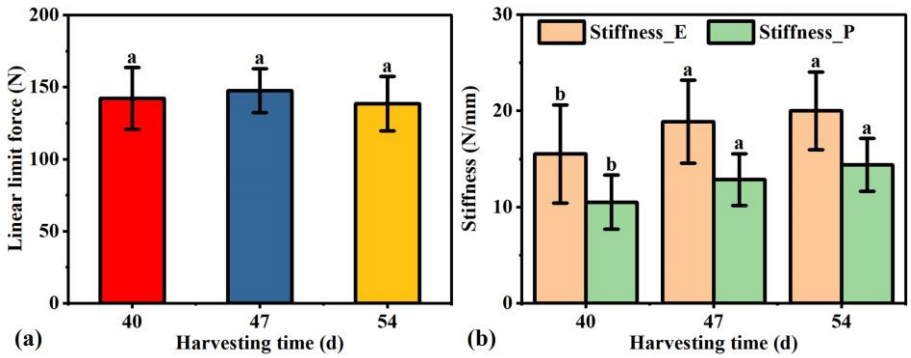

Fig. 5. Compression feature measurements. Variation of (a) linear limit force and (b) stiffness, including Stiffness_E and Stiffness_P. (Appear in color online only)

3.1.3 Texture indices

The maximum cutting force for the cabbage samples was recorded as the texture indices of laminas and midribs at three harvesting times (Fig. 6). Overall, the texture indices of laminas and midribs exhibit a consistent upward trend with advancing harvesting time. This indicates a significant increase in texture indices throughout the harvest period, which is also revealed by the acoustical vibration method (Taniwaki et al., 2009). The disparity in texture indices between midribs at 40 d and 47 d is not particularly obvious, while a significant difference is observed in the texture indices between 47 d and 54 d, excluding $F_{Lamina\ 3}$. Moreover, texture indices of laminas exhibit a noticeable difference between 40 d and 47 d, which confirms again that harvesting time can serve as a distinguishing factor for texture indices (Taniwaki et al., 2009). The outer leaves exhibit higher texture indices values compared to the inner leaves, and the texture indices of midribs are significantly higher than those of laminas. The maximum texture indices recorded for these samples are 17.89 N in lamina 1 (the outermost lamina harvested at 54 d, as depicted in Fig 6a) and 37.03 N in midrib 1 (the outermost midrib harvested at 54 d, as shown in Fig 6b). The reason is that the midribs between laminas typically contain several to many discrete and scattered veins arising independently within the atactostele (Keating, 2002), and the midribs have greater size and weight compared to the laminas, hence necessitating more energy for cutting. Consequently, the texture indices of the midribs are higher than those of the laminas in the same harvesting time.

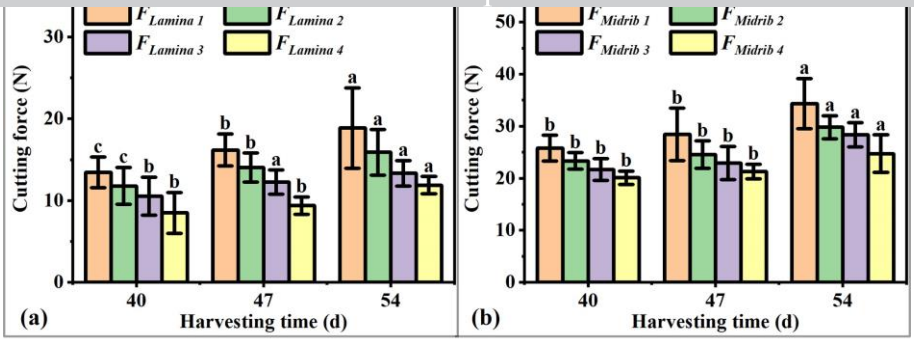

Fig. 6. Texture index measurements. Variation of (a) lamina cutting peak force and (b) midrib cutting peak force. (Appear in color online only)

3.2 Correlations among morphological traits, compression features, and textural indices

CA and APLSR were applied to reveal the correlations among morphological traits, compression features, and texture indices, and the results are presented in Figs. 7 and 8. The results of CA, as depicted in Fig. 7, highlight the morphological traits are found to be positively correlated with texture indices of laminas and midribs with a significant difference. Regarding the compression features (highlighted in the red rectangle), they exhibit a weaker correlation with the texture indices compared to the morphological traits. The correlation coefficients for these features were all below 0.35.

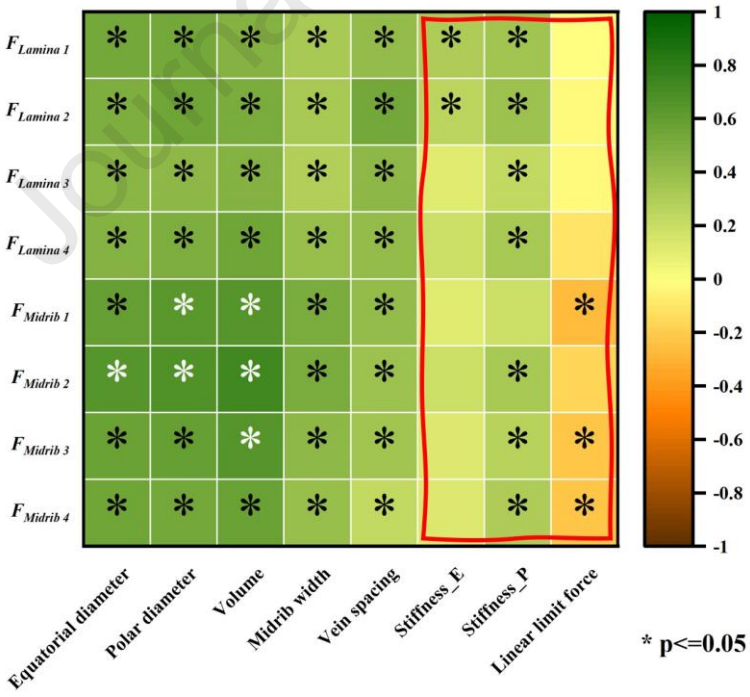

Fig. 7. Correlation analysis results based on Pearson correlation analysis method. The red rectangle marked part represents the correlation results between compression features and texture indices. (Appear in color online only)

APLSR was also applied to visualize the correlations among morphological traits, compression features, and texture indices, and the results are presented in Fig. 8.

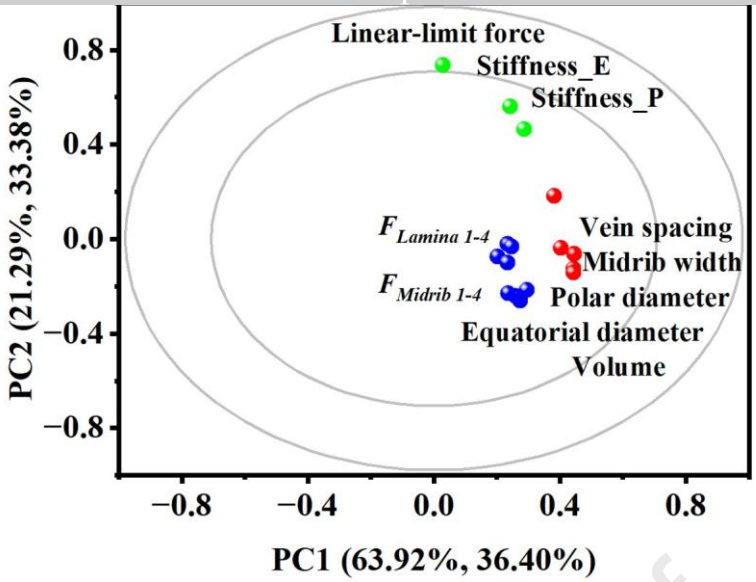

319

320 *Fig. 8. Correlation loadings plot for morphological traits and compression parameters (X-matrix) and texture indices (Y-*
321 *matrix) using APLSR. The concentric small and big ellipses show a confidence coefficient of 50% and 100% explained*
322 *variance, respectively. (Appear in color online only)*

323 Morphological traits and compression features were assigned by the X-matrix, while the texture indices were assigned
324 by the Y-matrix. The derived APLSR model included two significant PCs (PC1 and PC2) that explained 85.21% of the
325 variance in X-matrix and 69.78% of the variance in Y-matrix. The small ellipse shown in Fig. 8 represents a 50% confidence
326 coefficient of the variance, while the big one represents 100%. The closer the two variables are to each other, the higher their
327 correlation. Both the compression features and morphological traits are observed to have inadequate explanations by the two
328 PCs. However, the morphological traits exhibit a better correlation with the texture indices compared to the compression
329 features. The reason is that the texture of leafy vegetables is predominantly influenced by the physical anatomy of the tissue,
330 particularly cell size, shape and packing, cell wall thickness and strength, and turgor status (Toivonen and Brummell, 2008).
331 And the physical anatomy of the tissue has a significant impact on the morphology of the vegetables, including their size and
332 vein distribution (de la Riva et al., 2016). Consequently, texture indices exhibit a strong correlation with morphological traits
333 in cabbages, but display a weak correlation with compression features. Therefore, morphological traits would serve as more
334 effective characteristics for texture evaluation, outperforming the compression features.

335 *3.3 Texture quality prediction*

336 Considering the results of correlation analysis, morphological traits were used as the independent variables to establish

the detailed function relationship with texture indices by PLSR, PR, SVR, and XGBoostR algorithm, and the results are shown in Fig. 9 and listed in Tables A.1, A.2, A.3 and A.4 (Supplementary Data 1).

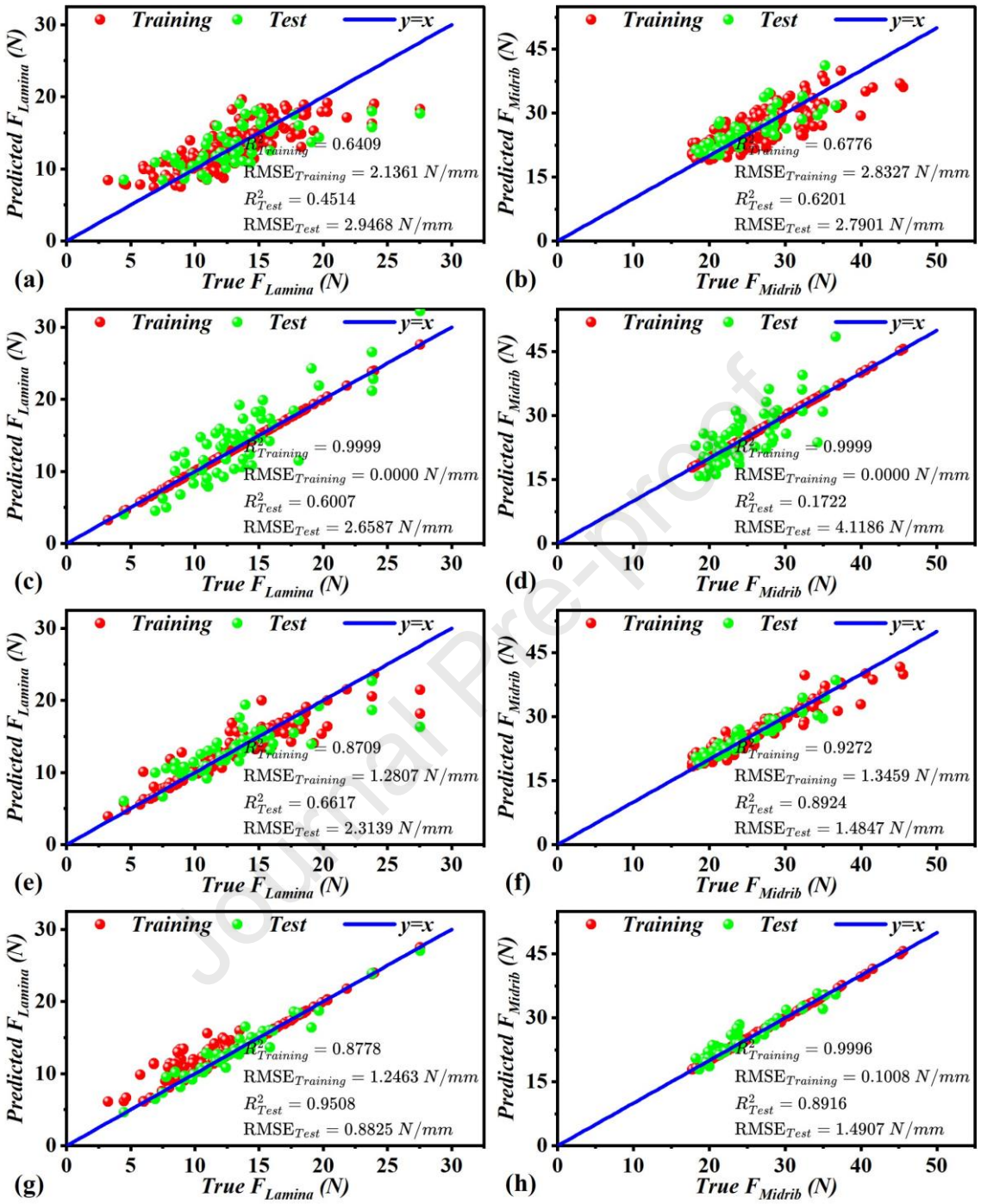

Fig. 9. Texture indices prediction. Lamina texture quality prediction obtained by (a) PLSR, (c) PR, (e) SVR, and (g) XGBoostR, and midrib texture quality prediction obtained by (b) PLSR, (d) PR, (f) SVR, and (h) XGBoostR. (Appear in color online only)

As shown in Figs. 9a and 9b and Table A.1, PLSR shows bad prediction performance in both training and test sets, with all R^2 values being less than 0.70. The R^2 values of F_{Lamina} in test sets are all below 0.2 due to the significant data pair differences, indicating this linear-fitting method is not suitable. For the nonlinear PR prediction shown in Figs. 9c and 9d and

Table A.2, the good performance of curve fitting in the training set is achieved, but the prediction effects in the test set deteriorate rapidly. Especially for the texture indices of the midrib, the R^2 values are all less than 0.6. The reason is that this model is overfitted with a small amount of training data. For SVR prediction shown in Figs .9e and 9f and Table A.3, the performance of midrib texture indices is better than the laminas texture indices in both training and test sets, with R^2 scores exceeding 0.89 and RMSE values below 1.5 N/mm. The laminas texture prediction exhibits excellent performance in the training set, boasting an impressive R^2 value of over 0.87. However, things take a downturn in the test set, where the results show a decline with an R^2 score falling below 0.70. Compared with SVR, XGBoostR achieves almost the same performance in midrib texture indices prediction and better performance in laminas texture indices prediction. Considering the accuracy shown in Figs. 9g and 9h and Table A.4, the morphological traits, when employed with XGBoostR, exhibit impressive predictive capabilities for the texture indices of laminas and midribs. The lamina texture indices achieve a remarkable prediction performance with an R^2 of 0.9508 and an RMSE of 0.8825 N/mm. Similarly, the midrib texture indices result in a good prediction performance with an R^2 of 0.8916 and an RMSE of 1.4907 N/mm. The performance of lamina texture in prediction is superior to that of midrib texture. The highest prediction performance is observed for $F_{Lamina\ 1}$ (R^2 = 0.9999 in the training set, R^2 = 0.9913 in the test set) and $F_{Midrib\ 1}$ (R^2 = 0.9992 in the training set, R^2 = 0.9217 in the test set), respectively. The results conclusively indicate that the texture quality of cabbages can be accurately predicted by leveraging the combination of morphological traits and advanced machine learning algorithms.

3.4 Texture quality discrimination

Texture quality discrimination of the cabbage samples at three harvest times was visualized through PCA and LDA, utilizing the morphological traits. The first two principal components (PCs), PC1 and PC2, were utilized to obtain the scoring and loading map of the texture quality. According to the score results of PCA in Fig.10a, the first two PCs explain 93.26% of the total variance (PC1=86.34% and PC2=6.92%). The cabbage samples are successfully divided into three distinct groups using the PCA algorithm, which corresponds to the harvesting time. Interestingly, the samples harvested at 40 d show obvious differentiation from those harvested at 47 d and 54 d. However, there is a considerable overlap observed between the cabbage samples harvested at 47 d and 54 d. The PCA loading plot indicates that when a variable's loading value is closer to the origin, it signifies that the variable had minimal influence on the corresponding PCs, and vice versa. Considering the prior knowledge

provided by the unsupervised PCA for the discrimination of texture quality, the supervised LDA was further employed for discrimination. As depicted in Fig. 10 (b), the PCA loading results indicate that the vein spacing emerges as the predominant factor influencing the discrimination. The discrimination results by LDA are superior to those by PCA. According to the LDA results in Fig.10c, the sum of the first two linear discriminants (LDs), LD1 and LD2, explains 100% of the total variance (LD1 = 93.61% and LD2 = 6.39%). Furthermore, it is found that the samples could also be successfully discriminated into three groups by the LDA algorithm. The three groups are almost completely distinct with only a single overlap, and the samples within each group exhibit higher concentrations compared to the PCA score results. Moreover, the variation of samples between 40 d and 47 d is significantly larger than that observed in the PCA score plot. As a result, 98.33% of the training samples and 100% of the test samples are correctly discriminated by the LDA algorithm (Fig. 10d). Only one sample is mistakenly classified in the harvesting period from 54 d to 47 d. In previous studies, machine vision was commonly employed to extract morphological traits, which were subsequently utilized for the recognition of texture quality in other leafy vegetables such as broccoli (Kusumam et al., 2017) and lettuce (Birrell et al., 2020), enabling the discrimination of vegetable samples harvested at different times. This proposed 3D scanning method would provide another approach to recognizing the texture quality of leaf vegetables by extracting the geometrical traits combined with surface features related to vein distribution.

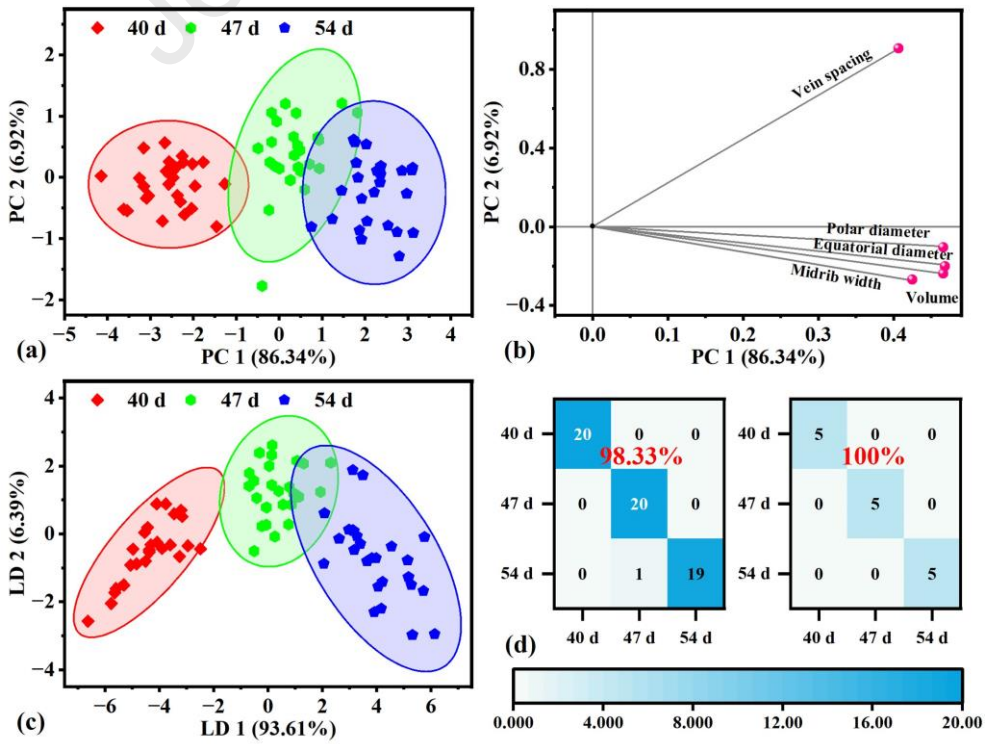

Fig. 10. Texture indices discrimination. Texture quality discrimination score plot obtained by (a) PCA and (c) LDA. (b) PCA texture quality discrimination loading plot. (d) Confusion matrix heatmap of the training set (left) and test set (right) obtained by LDA. (Appear in color online only)

4 Conclusion

In this study, a nondestructive method based on 3D scanning technology for determining the texture quality of leafy vegetables was proposed, using the harvested cabbages as experimental samples. The method allowed the extraction of the morphological traits of cabbages, including geometrical traits and vein distribution. The morphological traits were better correlated with texture indices of both laminas and midribs, compared to the compression features. Predicted results based on the XGBoostR algorithm revealed that the texture indices of laminas and midribs can be well predicted by morphological traits, where the prediction of lamina texture performed better than the midrib texture. In addition, the cabbage samples at different harvesting times can be successfully discriminated by morphological traits based on the LDA algorithm. These results indicated that 3D scanning technology is a promising approach for determining the texture quality of cabbages. Future works would develop grading devices in the cabbage production line using 3D scanners, providing new approaches for online processing equipment to evaluate the texture quality of the leafy vegetables.

CRediT authorship contribution statement

Dongdong Du: Conceptualization, Data curation, Formal analysis, Investigation, Methodology, Writing - original draft, Writing - review & editing, Software. **Yongkai Ye:** Writing - review & editing, Software. **Dongfang Li:** Writing - review & editing, Software. **Jie Fan:** Writing - review & editing. **Rob B.N. Scharff:** Writing - review & editing, **Jun Wang:** Writing - review & editing, Supervision. **Fake Shan:** Methodology.

Declaration of competing interest

The authors declare that they have no known competing financial interests or personal relationships that could have appeared to influence the work reported in this paper.

Funding

This work was supported by the National Natural Science Foundation of China (Grant Number 32301709), the Natural Science Foundation of Zhejiang Province (Grant Number Q21C130037), and the Zhejiang Agricultural Cooperation

Agreement (Grant Number 2023SNJF047).

Appendices A. Supplementary data

Supplementary Data 1

References

Adamczak, L., Chmiel, M., Florowski, T., Pietrzak, D., Witkowski, M., & Barczak, T. (2015). A potential use of 3-D scanning to evaluate the chemical composition of pork meat. *Journal of Food Science* 80(7), E1506-E1511. https://doi.org//10.1111/1750-3841.12913.

Adamczak, L., Chmiel, M., Florowski, T., Pietrzak, D., Witkowski, M., & Barczak, T. (2018). The use of 3D scanning to determine the weight of the chicken breast. *Computers and Electronics in Agriculture* 155, 394-399. https://doi.org//10.1016/j.compag.2018.10.039.

Awad, M., & Khanna, R. (2015). Support Vector Regression. *Efficient Learning Machines: Theories, Concepts, and Applications for Engineers and System Designers*, 67-80. https://doi.org//10.1007/978-1-4302-5990-9_4.

Bergstra, J., & Bengio, Y. (2012). Random search for hyper-parameter optimization. *Journal of Machine Learning Research* 13, 281-305. https://doi.org//10.5555/2188385.2188395.

Birrell, S., Hughes, J., Cai, J.Y., & Iida, F. (2020). A field-tested robotic harvesting system for iceberg lettuce. *Journal of Field Robotics* 37(2), 225-245. https://doi.org//10.1002/rob.21888.

Chen, T., & Guestrin, C. (2016). XGBoost: A Scalable Tree Boosting System. *Proceedings of the 22nd ACM SIGKDD International Conference on Knowledge Discovery and Data Mining*, 785–794. https://doi.org//10.1145/2939672.2939785.

Choong, M.F., Lucas, P.W., Ong, J.S.Y., Pereira, B., Tan, H.T.W., & Turner, I.M. (1992). Leaf fracture toughness and sclerophylly: their correlations and ecological implications. *New Phytologist* 121(4), 597-610. https://doi.org//10.1111/j.1469-8137.1992.tb01131.x.

de la Riva, E.G., Olmo, M., Poorter, H., Ubera, J.L., & Villar, R. (2016). Leaf mass per area (LMA) and Its relationship with leaf structure and anatomy in 34 mediterranean woody species along a water availability gradient. *PLOS ONE* 11(2), e0148788. https://doi.org//10.1371/journal.pone.0148788.

Dean, A., Voss, D., & Draguljić, D. (2017). Polynomial Regression. *Design and Analysis of Experiments*, 249-284. https://doi.org//10.1007/978-3-319-52250-0_8.

Fathizadeh, Z., Aboonajmi, M., & Beygi, S.R.H. (2020). Nondestructive firmness prediction of apple fruit using acoustic vibration response. *Scientia Horticulturae* 262, 109073. https://doi.org//10.1016/j.scienta.2019.109073.

Geng, J. (2011). Structured-light 3D surface imaging: a tutorial. *Advances in Optics and Photonics* 3(2), 128-160. https://doi.org//10.1364/AOP.3.000128.

Gil, M., Tudela, J., Martínez-Sánchez, A., & Luna, M. (2012). Harvest maturity indicators of leafy vegetables. *Stewart Postharvest Review* 8(1), 1-9. https://doi.org//10.2212/spr.2012.1.2.

Gonzalez, R.C., Woods, R.E., & Eddins, S.L. (2004). *Digital Image Processing Using MATLAB*. Pearson Prentice Hall, Upper Saddle River, NJ, USA.

Gu, S., Wang, J., & Wang, Y. (2019). Early discrimination and growth tracking of Aspergillus spp. contamination in rice kernels using electronic nose. *Food Chemistry* 292, 325-335. https://doi.org//10.1016/j.foodchem.2019.04.054.

Guebel, D.V., & Torres, N.V. (2013). Partial Least-Squares Regression (PLSR). *Encyclopedia of Systems Biology*, 1646-1648. https://doi.org//10.1007/978-1-4419-9863-7_1274.

Gutiérrez-Rodríguez, E., Lieth, H.J., Jernstedt, J.A., Labavitch, J.M., Suslow, T.V., & Cantwell, M.I. (2013). Texture, composition and anatomy of spinach leaves in relation to nitrogen fertilization. *Journal of the Science of Food and Agriculture* 93(2), 227-237. https://doi.org//10.1002/jsfa.5780.

Han, C., Choi, H., Jo, S., Na, H., Kim, M.K., Kim, M.-J., & Lee, J. (2020). Development of a 3D scanning method to discriminate blocks of Octopus minor with surplus water gain. *Food Chemistry* 303, 125414. https://doi.org//10.1016/j.foodchem.2019.125414.

Holt, J.E., & Schoorl, D. (1983). Cracking and enegry dissipation in cabbages. *Journal of Texture Studies* 14(2), 99-111.

https://doi.org/10.1111/jfpe.13802.

Jaiswal, A.K., & Abu-Ghannam, N. (2013). Degradation kinetic modelling of color, texture, polyphenols and antioxidant capacity of York cabbage after microwave processing. *Food Research International* 53(1), 125-133. https://doi.org//10.1016/j.foodres.2013.04.007.

Jaiswal, A.K., Gupta, S., & Abu-Ghannam, N. (2012). Kinetic evaluation of colour, texture, polyphenols and antioxidant capacity of Irish York cabbage after blanching treatment. *Food Chemistry* 131(1), 63-72. https://doi.org//10.1016/j.foodchem.2011.08.032.

Jang, T.Y., Hwang, S.S., Kim, H.-D., & Kim, S.-D. (2014). Bounding volume estimation algorithm for image-based 3D object reconstruction. *IEIE Transactions on Smart Processing and Computing* 3, 59-64. https://doi.org//10.5573/IEIESPC.2014.3.2.59.

Ji-Shi, A., Tian, L., Zhao, W., & Zhao, J. (2024). Elevational variations of leaf morphological traits and its responses to simulated climate warming in Tibetan alpine meadows. *Global Ecology and Conservation* 49, e02788. https://doi.org//10.1016/j.gecco.2023.e02788.

Keating, R.C. (2002). Leaf anatomical characters and their value in understanding morphoclines in the Araceae. *The Botanical Review* 68(4), 510-523. https://doi.org//10.1663/0006-8101(2002)068[0510:LACATV]2.0.CO;2.

Kusumam, K., Krajník, T., Pearson, S., Duckett, T., & Cielniak, G. (2017). 3D-vision based detection, localization, and sizing of broccoli heads in the field. *Journal of Field Robotics* 34(8), 1505-1518. https://doi.org//10.1002/rob.21726.

Li, Y., Zhao, H., Xiang, K., Li, D., Liu, C., Wang, H., Pang, W., Niu, L., Yu, R., & Sun, X. (2023). Factors affecting chemical and textural properties of dried tuber, fruit and vegetable. *Journal of Food Engineering*, 111828. https://doi.org//10.1016/j.jfoodeng.2023.111828.

Li, Z. (2013). The effect of compressibility, loading position and probe shape on the rupture probability of tomato fruits. *Journal of Food Engineering* 119(3), 471-476. https://doi.org//10.1016/j.jfoodeng.2013.06.024.

Liu, P., Zhang, P., Ni, F., & Hu, Y. (2021). Feasibility of nondestructive detection of apple crispness based on spectroscopy and machine vision. *Journal of Food Process Engineering*, e13802. https://doi.org//10.1111/jfpe.13802.

Macrelli, E., Romani, A., Paganelli, R.P., Sangiorgi, E., & Tartagni, M. (2013a). Piezoelectric transducers for real-time evaluation of fruit firmness. Part I: Theory and development of acoustic techniques. *Sensors and Actuators A: Physical* 201, 487-496. https://doi.org//10.1016/j.sna.2013.07.033.

Macrelli, E., Romani, A., Paganelli, R.P., Sangiorgi, E., & Tartagni, M. (2013b). Piezoelectric transducers for real-time evaluation of fruit firmness. Part II: Statistical and sorting analysis. *Sensors and Actuators A: Physical* 201, 497-503. https://doi.org//10.1016/j.sna.2013.07.037.

Mayorga-Martínez, A.A., Olvera-Trejo, D., Elías-Zúñiga, A., Parra-Saldívar, R., & Chuck-Hernández, C. (2016). Non-destructive assessment of guava (Psidium guajava L.) maturity and firmness based on mechanical vibration response. *Food and Bioprocess Technology* 9(9), 1471-1480. https://doi.org//10.1007/s11947-016-1736-8.

Otsu, N. (1979). A threshold selection method from gray-level histograms. *IEEE Transactions on Systems, Man, and Cybernetics* 9(1), 62-66. https://doi.org//10.1109/TSMC.1979.4310076.

Pullanagari, R.R., & Li, M. (2021). Uncertainty assessment for firmness and total soluble solids of sweet cherries using hyperspectral imaging and multivariate statistics. *Journal of Food Engineering* 289, 110177. https://doi.org//10.1016/j.jfoodeng.2020.110177.

Radovich, T.J.K., Kleinhenz, M.D., & Honeck, N.J. (2004). Important cabbage head traits and their relationships at five points in development. *Journal of Vegetable Crop Production* 10(2), 19-32. https://doi.org//10.1300/J068v10n02_03.

Retta, M.A., Verlinden, B., Verboven, P., & Nicolai, B. (2019). Texture-microstructure relationship of leafy vegetables during postharvest storage. *Acta horticulturae*, 169-178. https://doi.org//10.17660/ActaHortic.2019.1256.24.

Saeed, K., Tabędzki, M., Rybnik, M., & Adamski, M. (2010). K3M: A universal algorithm for image skeletonization and a review of thinning techniques. *Int. J. Appl. Math. Comput. Sci.* 20(2), 317–335. https://doi.org//10.2478/v10006-010-0024-4.

Sánchez, M.-T., Entrenas, J.-A., Torres, I., Vega, M., & Pérez-Marín, D. (2018). Monitoring texture and other quality parameters in spinach plants using NIR spectroscopy. *Computers and Electronics in Agriculture* 155, 446-452. https://doi.org//10.1016/j.compag.2018.11.004.

Satric, A., Tomasevic, I., Djekic, I., Pavlovic, V., Levic, S., & Miocinovic, J. (2024). Evaluation of low sodium Kačkavalj cheese properties using 3D scanning, scanning electron microscopy and computer vision system. *International Journal of Dairy Technology*. https://doi.org//10.1111/1471-0307.13046.

Tanwaki, M., Takahashi, M., Sakurai, N., Takada, A., & Nagata, M. (2009). Effects of harvest time and low temperature storage on the texture of cabbage leaves. *Postharvest Biology and Technology* 54(2), 106-110. https://doi.org//10.1016/j.postharvbio.2009.06.004.

Theodore, J.K.R., Matthew, D.K., & John, G.S. (2005). Irrigation timing relative to head development influences yield components, sugar levels, and glucosinolate concentrations in cabbage. *Journal of the American Society for Horticultural Science* 130(6), 943-949. https://doi.org//10.21273/JASHS.130.6.943.

Toivonen, P.M.A., & Brummell, D.A. (2008). Biochemical bases of appearance and texture changes in fresh-cut fruit and vegetables. *Postharvest Biology and Technology* 48(1), 1-14. https://doi.org//10.1016/j.postharvbio.2007.09.004.

Uyar, R., & Erdoğdu, F. (2009). Potential use of 3-dimensional scanners for food process modeling. *Journal of Food Engineering* 93(3), 337-343. https://doi.org//10.1016/j.jfoodeng.2009.01.034.

Watanabe, T., Ando, Y., Orikasa, T., Shiina, T., & Kohyama, K. (2017). Effect of short time heating on the mechanical fracture and electrical impedance properties of spinach (Spinacia oleracea L.). *Journal of Food Engineering* 194, 9-14. https://doi.org//10.1016/j.jfoodeng.2016.09.001.

Yu, X., Lu, H., & Wu, D. (2018). Development of deep learning method for predicting firmness and soluble solid content of postharvest Korla fragrant pear using Vis/NIR hyperspectral reflectance imaging. *Postharvest Biology and Technology* 141, 39-49. https://doi.org//10.1016/j.postharvbio.2018.02.013.

Zhang, J., Wang, J., Du, D., Zheng, C., Wang, Y., & Han, C. (2022). Evaluation of compactness as a method to quantitatively assess Chinese cabbage texture. *Postharvest Biology and Technology* 194, 112091. https://doi.org//10.1016/j.postharvbio.2022.112091.

Zhang, J., Wang, J., Zheng, C., Guo, H., & Shan, F. (2021). Nondestructive evaluation of Chinese cabbage quality using mechanical vibration response. *Computers and Electronics in Agriculture* 188, 106317. https://doi.org//10.1016/j.compag.2021.106317.

Zhang, W., Cui, D., & Ying, Y. (2015). Nondestructive Measurement of Texture of Three Pear Varieties and Variety Discrimination by the Laser Doppler Vibrometer Method. *Food and Bioprocess Technology* 8(9), 1974-1981. https://doi.org//10.1007/s11947-015-1547-3.

Highlights:

< Vein distribution of leafy cabbage was extracted using 3D scanning technology.

< Good correlations existed between morphological traits and texture.

< Morphological traits performed well in the texture quality evaluation.

Declaration of interests

☒ The authors declare that they have no known competing financial interests or personal relationships that could have appeared to influence the work reported in this paper.

☐The authors declare the following financial interests/personal relationships which may be considered as potential competing interests: